Phenylpyruvate Tautomerase Activity of *trans*-3-Chloroacrylic Acid Dehalogenase: Evidence for an Enol Intermediate in the Dehalogenase Reaction?†

Gerrit J. Poelarends,‡ William H. Johnson, Jr.,§ Hector Serrano,§ and Christian P. Whitman*,§

Department of Pharmaceutical Biology, Groningen Research Institute of Pharmacy, University of Groningen, Antonius Deusinglaan 1, 9713 AV Groningen, The Netherlands, and Division of Medicinal Chemistry, College of Pharmacy, The University of Texas, Austin, Texas 78712-1074

Received April 16, 2007; Revised Manuscript Received June 17, 2007

ABSTRACT: The enzymatic conversion of *cis*- or *trans*-3-chloroacrylic acid to malonate semialdehyde is a key step in the bacterial degradation of the nematocide 1,3-dichloropropene. Two mechanisms have been proposed for the isomer-specific hydrolytic dehalogenases, *cis*- and *trans*-3-chloroacrylic acid dehalogenase (*cis*-CaaD and CaaD, respectively), responsible for this step. In one mechanism, the enol isomer of malonate semialdehyde is produced by the α,β-elimination of HCl from an initial halohydrin species. Phenylenolpyruvate has now been found to be a substrate for CaaD with a k_{cat}/K_m value that approaches the one determined for the CaaD reaction using *trans*-3-chloroacrylate. Moreover, the reaction is stereoselective, generating the 3*S* isomer of [3-^{2}H]phenylpyruvate in a 1.8:1 ratio in ^2H_2O. These two observations and a kinetic analysis of active site mutants of CaaD suggest that the active site of CaaD is responsible for the phenylpyruvate tautomerase (PPT) activity. The activity is a striking example of catalytic promiscuity and could reflect the presence of an enol intermediate in CaaD-mediated dehalogenation of *trans*-3-chloroacrylate. CaaD and *cis*-CaaD represent different families in the tautomerase superfamily, a group of structurally homologous proteins characterized by a core β−α−β building block and a catalytic Pro-1. The eukaryotic immunoregulatory protein known as macrophage migration inhibitory factor (MIF), also a tautomerase superfamily member, exhibits a PPT activity, but the biological relevance is unknown. In addition to the mechanistic implications, these results establish a functional link between CaaD and the superfamily tautomerases, highlight the catalytic and binding promiscuity of the β−α−β scaffold, and suggest that the PPT activity of MIF could reflect a partial reaction in an unknown MIF-catalyzed reaction.

One reason for the persistence of halogenated organic compounds in the environment is the relative stability of the carbon−halogen bond (*1*). Nonetheless, microorganisms have generated enzymatic activities and assembled pathways that catabolize even some of the most recalcitrant of these compounds. In this context, it is notable that degradative pathways have evolved in various bacterial species (e.g., *Pseudomonas pavonaceae* 170 and coryneform bacterium strain FG41) to transform chlorinated alkenes such as the nematocide 1,3-dichloropropene (**1**, Scheme 1), and the *cis* and *trans* isomers of 3-chloroacrylic acid (**2** and **3**, respectively), into useful cellular metabolites (*1*−*5*). Accordingly, the isomeric mixture of **1** is first converted to **2** and **3** in three enzyme-catalyzed steps. Subsequently, isomer-specific 3-chloroacrylic acid dehalogenases process **2** (*cis*-CaaD)[1] or **3** (CaaD) to malonate semialdehyde (**4**), which is then decarboxylated by the action of malonate semialdehyde decarboxylase (MSAD) to yield acetaldehyde (**5**). Presumably, **5** is channeled into the Krebs cycle, allowing the organisms to use **1**−**3** as sources of carbon and energy.

Scheme 1

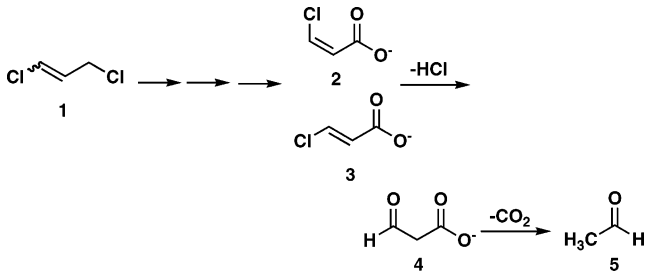

CaaD and *cis*-CaaD have received much scrutiny in recent years, and mechanisms for both enzymes have been formulated (*5*−*11*). The two enzymes are members of the tautomerase superfamily, a group of structurally homologous proteins characterized by a common β−α−β structural motif and a catalytic Pro-1 (*12*−*14*). In the proposed mechanism

† This research was supported by National Institutes of Health Grant GM-65324 and the Robert A. Welch Foundation (F-1334). G.J.P. was supported by a VENI grant from the Division of Chemical Sciences of the Netherlands Organization of Scientific Research (NWO-CW).

* To whom correspondence should be addressed. Telephone: (512) 471-6198. Fax: (512) 232-2606. E-mail: whitman@mail.utexas.edu.

‡ University of Groningen.

§ The University of Texas.

[1] Abbreviations: CaaD, *trans*-3-chloroacrylic acid dehalogenase; *cis*-CaaD, *cis*-3-chloroacrylic acid dehalogenase; DMSO, dimethyl sulfoxide; Kn, kanamycin; LB, Luria-Bertani; MSAD, malonate semialdehyde decarboxylase; MIF, macrophage migration inhibitory factor; 4-OT, 4-oxalocrotonate tautomerase; PPT, phenylpyruvate tautomerase; SDS−PAGE, sodium dodecyl sulfate−polyacrylamide gel electrophoresis.

10.1021/bi7007189 CCC: $37.00
Published on Web 07/28/2007

Scheme 2

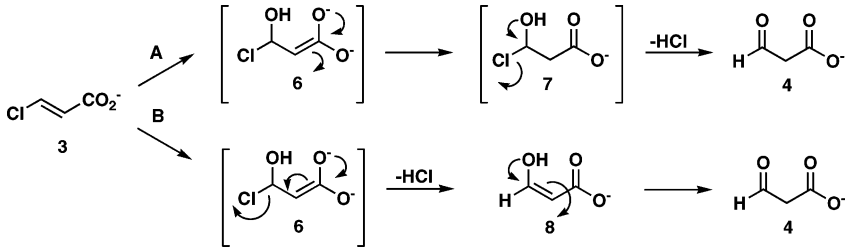

Scheme 3

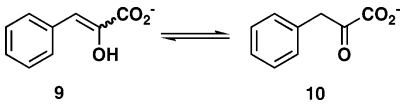

for the heterohexameric CaaD (Scheme 2), a water molecule is activated by αGlu-52 for addition at C-3 of **3**. Attack at C-3 is facilitated by two active site arginine residues (αArg-8 and αArg-11), which may interact with the carboxylate oxygens to activate the substrate and stabilize a proposed enediolate intermediate (**6**) (*5*−*8*). Two scenarios (routes A and B) can then be envisioned for **6**. In route A, **6** undergoes ketonization with protonation at C-2 by Pro-1 to produce an unstable halohydrin species (**7**). Direct explusion of the halide by an enzyme-catalyzed or a chemical process completes the reaction. In route B, ketonization of **6** eliminates the halide and produces the enol intermediate **8** (*8*, *11*). Tautomerization of the enol with protonation at C-2 by Pro-1 completes the transformation of **3** to **4**. Although the *cis*-CaaD mechanism involves two additional residues, it is proposed to proceed through a halohydrin or an enol intermediate, too (*11*).

Distinguishing between the two intermediates (i.e., **7** and **8**) is challenging but clearly has mechanistic implications as well as evolutionary significance. For example, a halohydrin intermediate could suggest that CaaD is an "accidental" dehalogenase in that the enzyme catalyzes a hydration reaction to form **7**, which can then undergo a very rapid chemical decay to yield **4**. In this scenario, the enzyme might function as a hydratase in the organism on an unknown physiological substrate (*14*). Alternatively, an enol intermediate suggests that CaaD evolved to carry out the dehalogenation reaction (i.e., it catalyzes an α,β-elimination reaction) and provides a functional link between CaaD and the tautomerases in the 4-oxalocrotonate tautomerase (4-OT) family.

In the course of examining substrates for CaaD, we found that it functions as an efficient phenylpyruvate tautomerase (PPT), converting phenylenolpyruvate (**9**, Scheme 3) to phenylpyruvate (**10**). Replacing βPro-1, αArg-8, or αArg-11 of CaaD with an alanine residue diminishes the PPT activity, whereas the αE52Q mutation has no effect on the PPT activity. These observations suggest that the PPT activity occurs in the active site and implicate βPro-1, αArg-8, and αArg-11 as participants in the activity. Furthermore, a stereochemical analysis of the reaction (in ^2H_2O) shows that CaaD produces the 3*S* isomer of [3-^{2}H]**10** in a ratio of ∼1.8:1, which is also consistent with the active site nature of the activity. The PPT activity of CaaD is a catalytically promiscuous activity, reflecting divergent evolution from an ancestral β−α−β template that likely gave rise to both CaaD and 4-OT. The activity also indicates that the active site of CaaD can ketonize enol compounds, thereby providing evidence for the presence of **6** in both mechanisms proposed for the CaaD-catalyzed reaction (routes A and B, Scheme 2) and for the presence of **8** in the mechanism shown in route B.

MATERIALS AND METHODS

Materials. Chemicals, biochemicals, buffers, and solvents were purchased from Sigma-Aldrich Chemical Co. (St. Louis, MO), Fisher Scientific Inc. (Pittsburgh, PA), Fluka Chemical Corp. (Milwaukee, WI), EM Science (Cincinnati, OH), or Acros Organics (Morris Plains, NJ). The Amicon stirred cells and the YM3 and YM10 ultrafiltration membranes were obtained from Millipore Co. (Billerica, MA). Prepacked PD-10 Sephadex G-25 columns were purchased from Biosciences AB (Uppsala, Sweden). Deoxyribonuclease (DNase) and ribonuclease (RNase) were purchased from F. Hoffmann-La Roche, Ltd. (Basel, Switzerland). All the enzymes used in this study were purified to near homogeneity, as assessed by sodium dodecyl sulfate−polyacrylamide gel electrophoresis (SDS−PAGE) on 15% gels (*15*).

General Methods. HPLC was performed on a Waters (Milford, MA) 501/510 system using either a TSKgel DEAE-5PW (anion exchange) or a TSKgel Phenyl-5PW (hydrophobic interaction) column (Tosoh Bioscience, Montgomeryville, PA). Protein concentrations were determined by the method of Waddell (*16*). Kinetic data were obtained on an Agilent 8453 UV−visible spectrophotometer. The kinetic data were fitted by nonlinear regression data analysis using Grafit (Erithacus, Software Ltd., Horley, U.K.) obtained from Sigma Chemical Co. Nuclear magnetic resonance (NMR) spectra were recorded in CD_3OD on a Varian UNITY-plus 300 MHz spectrometer or a Varian Unity INOVA-500 spectrometer. Chemical shifts are standardized to the CD_3-OD signal at 3.30 ppm.

Expression and Purification of CaaD, the CaaD Mutants (βP1A, αR8A, αR11A, and αE52Q), and cis-CaaD. The pET-24a(+) vector (Promega Corp., Madison, WI) used for the overexpression of CaaD was constructed and generously provided by J. E. Darty in our laboratory. The gene sequences for the α- and β-subunits of CaaD are separated by 13 bases in the pET3b vector and flanked by *Nde*I (5′-end) and *Bam*H1 (3′-end) restriction sites (*5*). Accordingly, the nucleotide sequence encoding the two genes was removed by treatment with the appropriate restriction enzymes and ligated into a similarly digested pET-24a(+) vector. Colonies containing pET-24a with the correct insert were identified, and plasmid DNA was isolated from a single colony selected from Luria-Bertani/kanamycin plates (LB/Kn, 50 μg/mL) and transformed into competent *Escherichia coli* BL21-Gold-

(DE3) cells (Stratagene, La Jolla, CA). CaaD was overexpressed using isopropyl β-D-thiogalactoside (1 mM). The enzyme was purified using published protocols (*6*−*8*), as modified below. Cells (∼5 g) from two 1 L cultures (grown on LB medium containing 50 μg/mL Kn) were suspended in ∼10 mL of 10 mM Na_2HPO_4 buffer (pH 8.0) (buffer A) along with DNase (10 μL of a 10 units/μL solution) and RNase (10 μL of a 500 μg/mL solution) and subjected to sonication. Subsequently, the mixture was centrifuged (45 min at 27000*g*), and the supernatant was filtered and loaded onto the TSKgel DEAE-5PW column, which had previously been equilibrated with buffer A. The column was washed using buffer A over a 10 min period at 5 mL/min. CaaD was eluted over a 60 min period using a linear Na_2SO_4 gradient (from 0 to 0.5 M). Typically, CaaD eluted from 9 to 34 min after being loaded onto the column. Fractions containing active CaaD were pooled and concentrated to ∼20 mL, and solid $(NH_4)_2SO_4$ was added to make the final concentration 1.0 M. After the mixture had been stirred for 1 h, the precipitate was removed by centrifugation (15 min at 27000*g*), and the supernatant was filtered and loaded onto the TSKgel Phenyl-5PW column, which had previously been equilibrated with buffer B [1.0 M $(NH_4)_2SO_4$ in 10 mM Na_2HPO_4 buffer (pH 8.0)]. The column was washed using buffer B over a 10 min period at 5 mL/min, and retained proteins were eluted with a decreasing linear gradient [from 1 to 0 M $(NH_4)_2SO_4$ in 10 mM Na_2HPO_4 buffer (pH 8.0)] over a 60 min period. Typically, CaaD eluted from 35 to 43 min. The appropriate fractions were pooled and concentrated to ∼5 mL, filtered through a 0.2 μm pore diameter filter, and stored at 4 °C. Typically, this protocol yields ∼40 mg of homogeneous protein per liter of culture. The four CaaD mutants were expressed constitutively using the pET3b vector transformed into competent *E. coli* BL21-Gold(DE3) cells. The construction of these mutants is described elsewhere (*5*, *8*). The mutants were purified using the protocol for the wild type, as decribed above. Likewise, *cis*-CaaD was expressed constitutively using the pET3b vector transformed into competent *E. coli* BL21-Gold(DE3) cells (*9*). The enzyme was purified following the protocol described above.

Expression and Purification of Macrophage Migration Inhibitory Factor (MIF). MIF-producing cells were grown, and the MIF was purified using protocols described elsewhere with the following modifications (*17*, *18*). Cells (∼4 g from 2 L of growth medium) were suspended in ∼10 mL of 10 mM NaH_2PO_4 buffer (pH 6.5) (buffer A), along with DNase and RNase at the concentrations indicated above, and disrupted by sonication. The lysed cells were centrifuged, and the supernatant was loaded onto the TSKgel DEAE-5PW column. After a 50 mL wash with the 10 mM NaH_2PO_4 buffer, the protein was eluted using a linear gradient (300 mL, from 0 to 0.5 M Na_2SO_4 in buffer A) at 5 mL/min. Typically, the protein eluted 8−15 min after being loaded onto the column. Pooled fractions were concentrated, made 1 M in $(NH_4)_2SO_4$, and loaded onto the TSKgel Phenyl-5PW column. After a 50 mL wash with 10 mM NaH_2PO_4 buffer containing 1 M $(NH_4)_2SO_4$, the protein was eluted using a linear gradient [250 mL, from 1 to 0 M $(NH_4)_2SO_4$ in 10 mM NaH_2PO_4 buffer (pH 6.5)] at 5 mL/min. Typically, the protein eluted from 63 to 70 min. Pooled fractions were concentrated to ∼7 mL, filtered through a 0.2 μm pore diameter filter, and stored at 4 °C. Under these conditions, 2 L of culture yields ∼50 mg of protein purified to near homogeneity (∼95% as assessed by SDS−PAGE).

Scheme 4

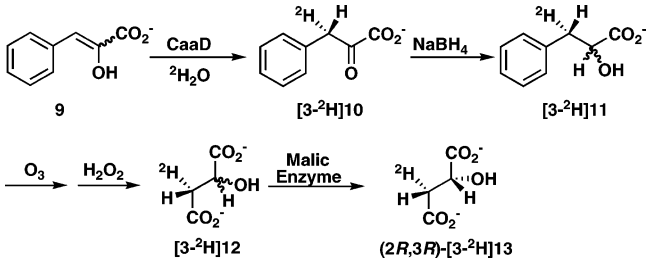

Kinetic Assays. The ketonization of phenylenolpyruvate (**9**) by MIF, CaaD, the four CaaD mutants, or *cis*-CaaD was monitored by following the depletion of the enol isomer (i.e., **9**) at 288 nm in 20 mM Na_2HPO_4 buffer at the indicated pH values (*19*). For MIF, the PPT activity was examined at pH 6.5, 6.8, 7.6, and 9.0. For CaaD, the PPT activity was examined at pH 6.5 and 9.0. The PPT activity of *cis*-CaaD and the four CaaD mutants was examined only at pH 9.0. An aliquot of each enzyme was diluted into 20 mL of 20 mM Na_2HPO_4 buffer at the desired pH, yielding various concentrations of MIF (0.01−0.025 μM), CaaD (0.3−13 μM), a CaaD mutant (0.9−15 μM), or *cis*-CaaD (18.5 μM). The diluted enzyme solutions were incubated for at least 60 min at 22 °C. Previous work has shown that the 1 h incubation period results in more reproducible kinetic data. Subsequently, 1 mL aliquots were transferred to a cuvette, and the assay was initiated by the addition of a small quantity (1−10 μL) of phenylenolpyruvic acid (**9**) from a 8 mM (MIF), 5 mM (CaaD and CaaD mutants), or 17.3 mM (*cis*-CaaD) stock solution. The stock solutions were made by dissolving the appropriate amount of phenylenolpyruvic acid in ethanol. The crystalline free acid of **9** is exclusively the enol form (*19*). In general, the concentrations of **9** used in the assay ranged from 0 to 80 μM (MIF), from 0 to 50 μM (CaaD and the CaaD mutants), and from 17.3 to 173 μM (*cis*-CaaD). At all substrate concentrations, the nonenzymatic rate was subtracted from the enzymatic rate of ketonization. The molar absorptivity coefficients (ε) were measured in 20 mM phosphate buffer adjusted to the pH used for the individual kinetic assays and ranged from 12 400 to 13 300 M^{-1} cm^{-1}. The kinetic parameters for CaaD and *cis*-CaaD using the appropriate isomer of 3-chloroacrylate (**2** or **3**) were determined by literature procedures (*6*, *9*).

*CaaD-Catalyzed Conversion of **9** to [3-^{2}H]**10** in D_2O and Conversion of [3-^{2}H]**10** to [3-^{2}H]**11***. The stereochemical analysis of [3-^{2}H]**10** was carried out by the series of reactions shown in Scheme 4 using protocols described elsewhere (*19*) with the following modifications. A total of 15 individual reaction mixtures was made up. A solution of **9** (4 mg, 24 mmol) dissolved in DMSO-d_6 (30 μL) was combined with a mixture of 100 mM Na_3PO_4 buffer made up in D_2O (225 μL, pH not adjusted) and 375 μL of D_2O. The addition of **9** (as the free acid) adjusted the pH to ∼9.0. Immediately thereafter, CaaD (50 μL of a 7.5 mg/mL solution) and a solution of $NaBH_4$ (50 μL of a 50 mg/mL solution in 20 mM NaH_2PO_4 buffer made up in D_2O) were added successively to the individual reaction mixtures. The reaction mixtures were then allowed to stand overnight at room temperature. Subsequently, the pH was adjusted to 1.9 using

aliquots of 8.5% H_3PO_4. The product, [3-^{2}H]**11**, was isolated as described previously (*19*) and purified using flash chromatography (2% acetic acid in ethyl acetate) to give 53.3 mg. The ^{1}H NMR spectrum corresponded to the previously reported one (*19*).

*Conversion of [3-^{2}H]**11** to (2R,3R)-[3-^{2}H]Malate (**13**).* The conversion of [3-^{2}H]**11** to **12** (Scheme 4) was carried out by the ozonolysis of [3-^{2}H]**11** (and treatment of the product with H_2O_2) to generate **12**, which was purified by anion exchange chromatography to afford 20.5 mg of product. The 2*S* isomer was removed by treating the diastereomeric mixture with malic enzyme as described previously (*19*) with the following modification. Commerically available malic enzyme was exchanged into 20 mM NaH_2PO_4 buffer (pH 7.4) (containing 5 mM $MgCl_2$) by gel filtration chromatography using a PD-10 Sephadex G-25 column. In the absence of this purification step, an unknown buffer component results in the degradation of **13** and significantly lowers the yield. The remaining 2*R* isomer was purified by anion exchange chromatography, yielding 6.2 mg of (2*R*,3*R*)-[3-^{2}H]malate (**13**). The ^{1}H NMR spectrum corresponded to the previously reported spectrum (*19*) and indicated that the 2*R*,3*R* isomer of [3-^{2}H]malate (**13**) predominated by a ratio of ~1.8:1.

*MIF-Catalyzed Conversion of **9** to [3-^{2}H]**10** in D_2O and Chemical and Enzymatic Conversion of [3-^{2}H]**10** to (2R,3S)-[3-^{2}H]Malate (**13**).* The stereochemical analysis of [3-^{2}H]-**10**, generated by the MIF-catalyzed ketonization of **9** in D_2O, was carried out by the same series of reactions shown in Scheme 4 as described above, but now using MIF (30 μL of an ~2.0 mg/mL solution) in place of CaaD. Ketonization, reduction with $NaBH_4$, and purification yielded 50.3 mg of [3-^{2}H]**11**. Ozonolysis of [3-^{2}H]**11**, treatment of the ozonide with H_2O_2, and purification afforded 15.5 mg of [3-^{2}H]**12**. Subsequent treatment with malic enzyme provided 5.1 mg of (2*R*,3*S*)-[3-^{2}H]malate (**13**). The ^{1}H NMR spectrum indicated that (2*R*,3*S*)-[3-^{2}H]malate (**13**) predominated by a ratio of ~6.6:1.

RESULTS

*Kinetic Parameters for the MIF- and CaaD-Catalyzed Ketonization of **9**.*[2] The kinetic parameters for the PPT activities of MIF and CaaD were measured under a variety of conditions, including different enzyme preparations and concentrations, different phosphate buffer concentrations (20 and 50 mM), and (for MIF) different pH values (6.5, 6.8, 7.6, and 9.0). Representative kinetic parameters for each reaction at the optimal pH value for the physiological reaction are summarized in Table 1. The kinetic parameters for the MIF-catalyzed reaction at pH 9.0 are also included.[3] The K_m values are comparable (within experimental error), but the k_{cat} values for the MIF-catalyzed reactions at pH 6.8 and 9.0 are 27- and 24-fold higher, respectively, than that measured for the CaaD-catalyzed reaction (using **9**). Primarily due to this difference, the k_{cat}/K_m values for the MIF-catalyzed reaction at pH 6.8 and 9.0 are 52- and 74-fold higher, respectively, than that measured for the CaaD-catalyzed reaction. The k_{cat}/K_m value for the CaaD-catalyzed reaction using **3**, the physiological substrate, is only ~3-fold higher than that for the CaaD-catalyzed reaction using **9**. Although there is some variation in the K_m and k_{cat} values under the assorted conditions described above, the k_{cat}/K_m values for the PPT activities range from $1-2 \times 10^6$ M^{-1} s^{-1} (for MIF) to $1-3 \times 10^4$ M^{-1} s^{-1} (for CaaD). The sum of these observations shows that CaaD has a robust PPT activity and it functions almost as efficiently as a PPT as it does a dehalogenase.

Table 1: Kinetic Parameters for MIF, CaaD, CaaD Mutants, and *cis*-CaaD[a]

enzyme	substrate	pH	K_m (μM)	k_{cat} (s^{-1})	k_{cat}/K_m (M^{-1} s^{-1})
MIF	**9**	6.8	31 ± 8	38 ± 4	1.2×10^6
MIF[b]	**9**	9.0	20 ± 8	33 ± 4	1.7×10^6
CaaD	**9**	9.0	61 ± 23	1.4 ± 0.3	2.3×10^4
CaaD	**3**	9.0	34 ± 2	2.4 ± 0.1	7.1×10^4
βP1A-CaaD	**9**	9.0	−	−	3×10^3
αR8A-CaaD	**9**	9.0	−	−	1.2×10^3
αR11A-CaaD	**9**	9.0	−	−	1.5×10^3
αE52Q-CaaD	**9**	9.0	113 ± 30	4.1 ± 1.0	3.6×10^4
cis-CaaD	**9**	9.0	110 ± 30	0.20 ± 0.03	1.8×10^3
cis-CaaD	**2**	9.0	34 ± 8	1.8 ± 0.2	5.3×10^4

[a] Assay conditions are provided in the text. [b] The kinetic parameters were measured in 50 mM Na_2HPO_4 buffer (pH 9.0).

*Kinetic Properties of the CaaD Mutants with **9**.* Kinetic, site-directed mutagenesis, NMR, and crystallographic analyses identified βPro-1, αArg-8, αArg-11, and αGlu-52 as four critical active site residues for CaaD activity (*5*−*8*). To establish the active site nature of the PPT activity of CaaD and to assess the importance of these four residues to the activity, the kinetic parameters for the ketonization of **9** by the βP1A, αR8A, αR11A, and αE52Q mutants were determined. The results are also summarized in Table 1. It was not possible to saturate the βP1A, αR8A, and αR11A mutants with **9**. Nonetheless, the three mutants exhibit approximately 8-, 19-, and 15-fold decreases, respectively, in their k_{cat}/K_m values compared to that determined for the wild-type enzyme. The K_m value for the αE52Q mutant is comparable (within experimental error) to that of the wild type, whereas the k_{cat} value is slightly higher (~3-fold) than that of wild-type CaaD. Overall, the k_{cat}/K_m value for the αE52Q-catalyzed reaction is also slightly higher (~1.6-fold) than that of the wild type. These observations suggest roles for βPro-1, αArg-8, and αArg-11 in the PPT activity of CaaD, but not for αGlu-52.

*Kinetic Parameters for the cis-CaaD-Catalyzed Ketonization of **9**.* The kinetic parameters for the PPT activity of *cis*-CaaD were also measured and compared to those measured for the PPT activity of MIF and the *cis*-CaaD reaction using **2** (Table 1). At pH 9.0, the K_m value for *cis*-CaaD (using **9**) is ~5.5-fold higher than that measured for MIF, but the k_{cat} value for the MIF-catalyzed reaction is ~165-fold higher than that measured for the same reaction catalyzed by *cis*-CaaD. As a result, the k_{cat}/K_m value for the MIF-catalyzed reaction is ~944-fold higher than that measured for the *cis*-CaaD-catalyzed reaction. The k_{cat}/K_m value for the *cis*-CaaD-catalyzed reaction using **2**, the physiological substrate, is ~29-fold higher than that of the *cis*-CaaD-catalyzed reaction using **9**. The results indicate that *cis*-CaaD

[2] The enzymatic activity of MIF is typically designated as the PPT activity of MIF. For simplicity of discussion, the enzymatic activity will occasionally be termed the MIF-catalyzed reaction.

[3] CaaD has little CaaD or PPT activity at pH 6.5 (k_{cat}/K_m values of <500 M^{-1} s^{-1}).

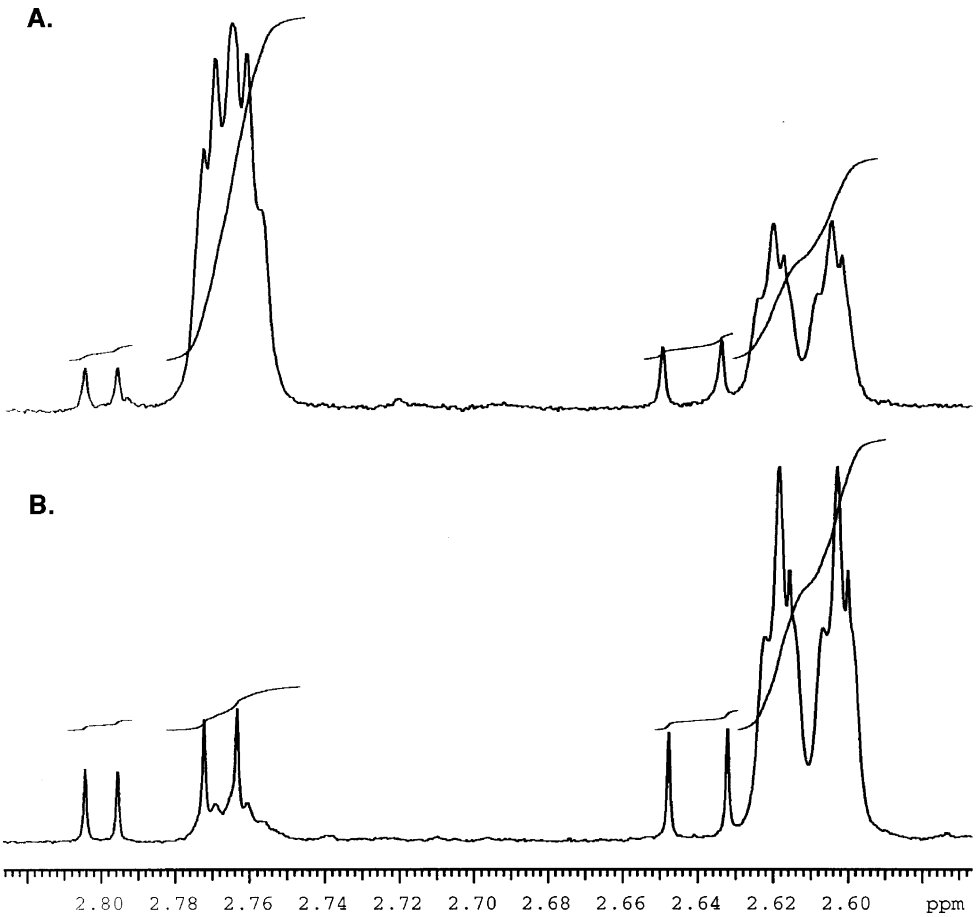

FIGURE 1: Partial ^{1}H NMR spectra (500 MHz, CD_3OD) of (2*R*)-[3-^{2}H]malate isolated in the stereochemical analysis of the (A) CaaD-catalyzed conversion of **9** to [3-^{2}H]**10** in ^2H_2O and (B) MIF-catalyzed conversion of **9** to [3-^{2}H]**10** in ^2H_2O. Both reactions were carried out at pH 9.0. The broadened doublet centered at 2.61 ppm corresponds to (2*R*,3*S*)-[3-^{2}H]malate (**13**), and the broadened doublet centered at 2.77 ppm corresponds to the (2*R*,3*R*)-[3-^{2}H]malate (*19*). The latter broadened doublet appears more like a broadened singlet due to the small coupling constant, which does not permit adequate resolution. For CaaD, the (2*R*,3*R*)-[3-^{2}H] isomer predominates by a ratio of ~1.8:1, as indicated by integration of the signals. For MIF, the (2*R*,3*S*)-[3-^{2}H] isomer predominates by a ratio of ~6.6:1. The less prominent doublets centered at 2.64, 2.77, and 2.80 ppm indicate the presence of fully protio malate.

has a PPT activity, but the activity is not as robust as that of CaaD.

*Stereochemical Analysis of the CaaD-Catalyzed Formation of [3-^{2}H]**10** from **9***. The CaaD-catalyzed ketonization of **9** was carried out in D_2O, and the product, [3-^{2}H]**10**, was trapped and analyzed as described elsewhere (*19*). The rapid chemical ketonization of **9** under these conditions [50 mM Na_2HPO_4 buffer (pH 9)] necessitated a major modification: the addition of enzyme was followed immediately by the addition of $NaBH_4$ in 15 small-scale reactions. The individual reactions increased the yield of stereoselectively labeled **10**. Accordingly, [3-^{2}H]**10** was converted by the series of chemical and enzyme-catalyzed reactions shown in Scheme 4 to the 2*R* isomer of [3-^{2}H]malate which was analyzed by ^{1}H NMR spectroscopy.

The C-3 protons of the fully protio malate are diastereotopic so that each proton gives rise to a doublet of doublets, one at ~2.62 ppm and the other at ~2.78 ppm (in CD_3OD) (*20*). The stereospecific incorporation of a deuteron results in the loss of one set of doublets and the collapse of the remaining set into a broadened doublet (*21*). Hence, the stereoselective incorporation of a deuteron results in two sets of broadened doublets, with one set predominating. It has been previously reported that a ^{1}H NMR spectrum of the 2*R*,3*R* isomer of [3-D]malate does not show the upfield signal (2.62 ppm) but does show a broadened doublet downfield (2.78 ppm) (*20*).

A partial ^{1}H NMR spectrum (recorded in CD_3OD) of the malate isolated from the CaaD-catalyzed reaction shows two major signals (Figure 1A). There is a broadened doublet centered at ~2.61 ppm, which corresponds to (2*R*,3*S*)-[3-^{2}H]**13**, and a broadened doublet centered at ~2.77 ppm, which corresponds to (2*R*,3*R*)-[3-^{2}H]**13** (Figure 1A). (The broadened doublet appears more like a broadened singlet due to the small coupling constant, which does not permit adequate resolution.) In addition, there are smaller doublets centered at 2.64 and 2.80 ppm, which correspond to fully protio malate resulting from the presence of H_2O in the reaction mixture. The height of the integral assigned to the 2*R*,3*R* isomer is ~1.8-fold greater than that of the corresponding integral for the 2*R*,3*S* isomer. The reaction is clearly stereoselective, and the 2*R*,3*R* isomer of [3-^{2}H]**13** predominates. The *R* configuration at C-3 of **13** indicates that the stereochemistry at C-3 of **10** is *S* because a phenyl group replaces the carboxylate group at C-4 (Scheme 5). On the basis of this assignment, CaaD catalyzes the ketonization of **9** to produce (3*S*)-[3-^{2}H]**10**, favoring the *S* isomer by a ratio of ~1.8:1.

A previous stereochemical analysis of the PPT activity of MIF was carried out at pH 6.8 (*19*). To provide a direct

Scheme 5

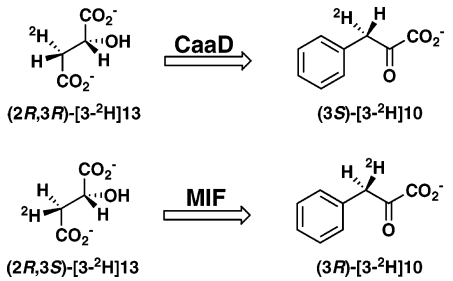

comparison between the CaaD- and MIF-catalyzed reactions, the stereochemical analysis of MIF was repeated at pH 9.0. Hence, the series of reactions described above was carried out using a comparable amount of MIF in place of CaaD. The ^{1}H NMR spectrum of the resulting 2*R* isomer of [3-^{2}H]-malate shows one major signal, that of a broadened doublet centered at ~2.61 ppm (Figure 1B). (Once again, there are smaller doublets centered at 2.64, 2.77, and 2.80 ppm, corresponding to the presence of fully protio malate.) The reaction is highly stereoselective with the 2*R*,3*S* isomer of [3-^{2}H]**13** predominating by a ratio of ~6.6:1, as assessed by integration of the signals. The *S* configuration at C-3 of **13** indicates that the stereochemistry at C-3 of **10** is *R* because a phenyl group replaces the carboxylate group at C-4 (Scheme 5). On the basis of this assignment, MIF catalyzes the ketonization of **9** to produce (3*R*)-[3-^{2}H]**10** by a ratio of ~6.6:1. This assignment is in accord with the results of the stereochemical analysis at pH 6.8. However, the reaction at pH 9.0 is less stereoselective than that at pH 6.8 (*19*). The loss of stereoselectivity is attributed to the faster chemical rate of ketonization at pH 9.0.

DISCUSSION

A PPT activity was first identified in various animal tissues in the 1950s, but there was no obvious physiological requirement for the activity (*22*). The protein was isolated and designated PPT. Knox and Pitt (*22*) suggested that PPT might play a role in the enol−keto tautomerization of α-keto acids because the chemical conversion of the enol to the keto form, particularly that of **9** to **10**, is slow. A later report proposed a role for PPT in the formation of the enol isomer of 4-hydroxy-3,5-diiodophenylpyruvate from the keto isomer in the thyroxine biosynthetic pathway (*23*, *24*). Despite sporadic mechanistic studies of PPT over the years (*25*, *26*), these observations have not been pursued further, and a physiological rationale for a PPT activity has never been firmly established.

In 1997, Rorsman and co-workers showed that PPT and MIF are identical proteins (*27*). MIF, first identified in the 1960s, is an important immunoregulatory protein that has been implicated in the pathogenesis of septic shock, arthritis, and other inflammatory conditions (*28*−*31*). The potential connection between the PPT activity and the biological activities of MIF ignited interest in defining a structural and mechanistic basis for the PPT activity so that this information could be used for the rational design of new anti-inflammatory agents (*32*, *33*). To date, an unequivocal connection between the PPT and biological activities remains elusive, but a better understanding of the mechanism for the PPT activity of MIF has emerged (*17*−*19*, *34*−*37*).

A crystal structure of the unliganded MIF placed the protein in the tautomerase superfamily (*35*, *36*). Kinetic, inhibition, and NMR studies implicated Pro-1 as the catalytic base (pK_a of ~5.6) (*37*), which abstracts the *pro-R* hydrogen of **10** (*25*). The highly stereoselective nature of the reaction (within the limits of detection) was reinforced by the finding that the ketonization of **9** in D_2O generates the 3*R* isomer of [3-D]**10** (*19*). Although the interconversion of **9** and **10** was thought to involve acid−base chemistry, an acid catalyst has not been identified (*34*). Moreover, site-directed mutagenesis experiments showed that only mutations of Pro-1 significantly impaired catalysis (*37*). On the basis of these observations, Stamps et al. (*34*) concluded that Pro-1 might act as both the acid and base catalyst.

We have now found that CaaD also displays a pronounced PPT activity. The activity approaches that observed for MIF as well as that of CaaD using **3**, and this kinetic competence could reflect the occurrence of enol intermediates (i.e., **6** or **8**) in the CaaD-catalyzed conversion of **3** to **4**. The CaaD-catalyzed ketonization of **9** is stereoselective, generating a mixture of stereosisomers of [3-D]**10** with the 3*S* isomer predominating. This observation is a compelling argument for an enzyme-catalyzed process and argues against a contaminating "MIF".[4] These results are even more remarkable in view of the fact that **9** is the "wrong" enol for the CaaD reaction, when compared to **8**. In addition to the phenyl ring, the 2-hydroxyl group is in the wrong position and the enol is likely a mixture of the 2*E* and 2*Z* isomers. These factors along with the rapid chemical rate of ketonization could easily account for the low stereoselectivity of the reaction. Overall, the results support a mechanism involving the α,*β*-elimination of HCl from the halohydrin species **6** to generate the enol of **4** (Scheme 2, route B). Subsequent ketonization of **8** produces **4**. Alternatively, these results may reflect the presence of **6** in both mechanisms.

As a result of the shared acrylate functionality, the binding of **9** at the active site of CaaD could parallel that proposed for **3** (*8*, *11*). In **3**, the carboxylate group of the substrate is presumed to interact with the αArg-8/αArg-11 pair while the remainder of the substrate projects deep into the active site formed, in part, by αPhe-39 and αPhe-50 (*8*, *11*). Likewise, the carboxylate group of **9** could interact with the αArg-8/αArg-11 pair, and the phenyl ring of **9** could interact with the αPhe-39/αPhe-50 pair. In this scenario, *β*Pro-1 could function as a general base and abstract the enol proton of **9**. The resulting conjugate acid could then deliver the proton to C-3 to yield **10**. Although *β*Pro-1 is thought to function as a general acid in the physiological reaction (i.e., using **3** as substrate) with a pK_a of ~9.2 (*7*), under the assay conditions (pH 9.0), a significant concentration of the enzyme exists in both the neutral (38.7%) and charged (61.3%) states. Whether this scenario parallels the proposed CaaD-catalyzed conversion of **8** to **4** is not known. It may be that another

[4] As an additional control experiment, a purified protein sample from cells harboring an "empty" pET-24a(+) vector (i.e., the genes encoding the CaaD subunits are absent) was examined. The extract from lysed transformed cells was subjected to the DEAE-5PW and Phenyl-5PW columns. Fractions corresponding to those where CaaD typically elutes were collected and concentrated to ~2−4 mL. An aliquot (1 mL) was diluted 20-fold. There was no significant PPT activity using 1 mL of this sample (G. J. Poelarends, W. H. Johnson, Jr., H. Serrano, and C. P. Whitman, 2007, unpublished results).

group functions as the general base and abstracts the enol proton of **8**.

The rate acceleration of the nonenzymatic reaction is another measure of catalytic efficiency. The uncatalyzed rate of hydration for **3** is $\sim 2.2 \times 10^{-12}$ s^{-1} at 25 °C (*38*). With a k_{cat} value of 2.4 s^{-1} (Table 1), CaaD affords a 10^{12}-fold rate enhancement (*39*). The uncatalyzed rate for the ketonization of **9** has not been reported. However, Peliska and O'Leary (*40*) determined that the uncatalyzed ketonization of enolpyruvate proceeds at a rate of $\sim 2.0 \times 10^{-3}$ s^{-1}. Using this value and the k_{cat} values reported for CaaD and MIF in Table 1 (at pH 9), it can be estimated that CaaD affords a 700-fold rate enhancement and MIF affords a 16500-fold rate enhancement. Although the actual rate enhancements are likely to be greater (i.e., **9** is more stable than enolpyruvate), CaaD is much more efficient as a dehalogenase than as a tautomerase using this standard of catalytic efficiency.

Assuming **9** and **3** bind similarly in the active site of CaaD, the decrease in PPT activity (as assessed by k_{cat}/K_m values) observed for three active site mutants is not particularly noteworthy, although the three mutant enzymes could not be saturated with substrate. These results are not, however, surprising in view of the studies on the PPT activity of MIF, which showed that the enzymatic activity is impaired only by mutations of Pro-1, and that the P1G and P1A mutants of MIF, for example, still have significant PPT activity (*34*, *37*). Both the P1G and P1A mutants of MIF exhibit a ~230-fold decrease in k_{cat}/K_m compared to that observed for the wild-type reaction (*34*). Likewise, the βP1A mutant of CaaD retains substantial PPT activity using **9**, which might be attributed to opposing effects of changing the βPro-1 to an alanine. Assuming the change in pK_a for the βAla-1 mutant parallels the difference in pK_a between proline and alanine (0.7 unit), the pK_a for the βP1A mutant is estimated to be 8.5 (*37*, *41*). Hence, at pH 9.0, more enzyme is in a neutral state (~76%) and the lowered basicity would be expected to increase activity (*37*, *41*). However, the conformational flexibility of the alanyl nitrogen compared to that of the constrained prolyl nitrogen would seemingly preclude effective abstraction of the enol proton and decrease the activity (*37*, *41*). Evidently, the increased flexibility of the base overrides the effect of the lowered basicitiy such that an overall decrease in activity is observed.

Our results also show that removing either of the active site arginines has a comparable effect on the k_{cat}/K_m value. It is possible that a single arginine is sufficient for binding the carboxylate group of **9** and that a major binding interaction could be one between the phenyl ring of **9** and the αPhe-39/αPhe-50 pair. The effects of mutations at these positions on the PPT activity of CaaD are under investigation. Finally, αGlu-52 is clearly not involved in binding or catalysis because replacing it with a glutamine has no significant effect on the PPT activity.

cis-CaaD also has a PPT activity, but it is lower than that of CaaD. The lower activity is not surprising in view of the different substrate specificities of the two enzymes (*11*). Crystallographic analysis suggests that the binding pocket of CaaD is more elongated whereas the pocket of *cis*-CaaD is more U-shaped (*11*). Accordingly, the active site of CaaD might better accommodate the bulkier phenyl group of **9** than does the active site of *cis*-CaaD. Nonetheless, the observation of a PPT activity suggests that the active site of *cis*-CaaD is also set up to ketonize enol compounds, and the dehalogenase reaction could proceed through the α,β-elimination of HCl. Once again, these observations could also reflect the presence of **6** in both mechanisms.

Scheme 6

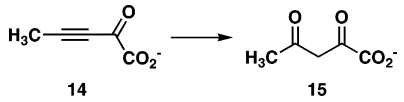

The PPT activity of CaaD is an impressive example of catalytic promiscuity. An ever growing body of work indicates that catalytic promiscuity plays a major role in the evolution of new enzymatic activities (*42*−*45*). The promiscuous template is presumed to require fewer mutations to "arrive" at a new activity, in contrast to the relatively large number of mutations (and accompanying deleterious consequences) that would be required for a template devoid of activity (*46*). Catalytic promiscuity is a common theme in the tautomerase superfamily, varying considerably in magnitude (*6*, *47*, *48*). In addition to the PPT activity, CaaD displays a robust hydratase activity (*6*) and a low-level MSAD activity (*47*). The hydratase activity was detected by the CaaD-catalyzed conversion of 2-oxo-3-pentynoate (**14**, Scheme 6) to acetopyruvate (**15**) and is ~19-fold lower than that of the wild-type reaction using **3** (as assessed by k_{cat}/K_m values) (*6*).

Among the tautomerases, 4-OT and YwhB, a closely related 4-OT homologue found in *Bacillus subtilis*, exhibit low-level CaaD activities (*47*). These observations established a functional link between the tautomerases and the dehalogenases (*47*). The observation of a PPT activity for CaaD now establishes a functional link between CaaD and the tautomerases. Nature clearly capitalized on the catalytic and binding promiscuity of the $\beta-\alpha-\beta$ fold for the diversification of enzyme function within the tautomerase superfamily and perhaps made advantageous use of the promiscuous hydration [conversion of **3** to **6** (Scheme 2)] and tautomerization [conversion of **8** to **4** (Scheme 2)] activities in the evolution of CaaD.

Finally, CaaD is the third tautomerase superfamily member to exhibit a significant PPT activity. MIF and YwhB are the other two (*49*). YwhB functions as a nonspecific tautomerase and lacks a genomic or pathway context (*49*). The k_{cat}/K_m values for the PPT activity ($\sim 4.2 \times 10^5$ M^{-1} s^{-1}) is between those observed for MIF and CaaD, and the 3*R* isomer of [3-D]**10** predominates in a ratio of 3:1.[5] In the absence of the genomic and pathway context, CaaD might have been misannotated as a PPT on the basis of its sequence similarity to the 4-OT family and its PPT activity. This raises the question of whether MIF and YwhB carry out other enzymatic reactions where the ketonization of an enol intermediate is one step in the overall reaction. With the discovery of more tautomerase superfamily activities, it may be possible to answer this question.

ACKNOWLEDGMENT

We thank Steve D. Sorey (Department of Chemistry, The University of Texas) for his assistance in acquiring the NMR

[5] S. C. Wang, W. H. Johnson, Jr., R. M. Czerwinski, S. L. Stamps, and C. P. Whitman, 2007, unpublished results.

spectra. We also thank Joseph E. Darty for the gift of the pET-24a(+) construct containing the genes for CaaD.

REFERENCES

1. Copley, S. D. (1999) Microbial dehalogenases, in *Comprehensive Natural Products Chemistry* (Barton, D., and Nakanishi, K., Eds.) Vol. 5, pp 401−422, Elsevier, Amsterdam.
2. Hartmans, S., Jansen, M. W., van der Werf, M. J., and de Bont, J. A. M. (1991) Bacterial metabolism of 3-chloroacrylic acid, *J. Gen. Microbiol. 137*, 2025−2032.
3. van Hylckama Vlieg, J. E. T., and Janssen, D. B. (1992) Bacterial degradation of 3-chloroacrylic acid and the characterization of *cis*- and *trans*-specific dehalogenases, *Biodegradation 2*, 139−150.
4. Poelarends, G. J., Wilkens, M., Larkin, M. J., van Elsas, J. D., and Janssen, D. B. (1998) Degradation of 1,3-dichloropropene by *Pseudomonas cichorii* 170, *Appl. Environ. Microbiol. 64*, 2931−2936.
5. Poelarends, G. J., Saunier, R., and Janssen, D. B. (2001) *trans*-3-Chloroacrylic acid dehalogenase from *Pseudomonas pavonaceae* 170 shares structural and mechanistic similarities with 4-oxalocrotonate tautomerase, *J. Bacteriol. 183*, 4269−4277.
6. Wang, S. C., Person, M. D., Johnson, W. H., Jr., and Whitman, C. P. (2003) Reactions of *trans*-3-chloroacrylic acid dehalogenase with acetylene substrates: Consequences of and evidence for a hydration reaction, *Biochemistry 42*, 8762−8773.
7. Azurmendi, H. F., Wang, S. C., Massiah, M. A., Poelarends, G. J., Whitman, C. P., and Mildvan, A. S. (2004) The roles of active-site residues in the catalytic mechanism of *trans*-3-chloroacrylic acid dehalogenase: A kinetic, NMR, and mutational analysis, *Biochemistry 43*, 4082−4091.
8. de Jong, R. M., Brugman, W., Poelarends, G. J., Whitman, C. P., and Dijkstra, B. W. (2004) The X-ray structure of *trans*-3-chloroacrylic acid dehalogenase reveals a novel hydration mechanism in the tautomerase superfamily, *J. Biol. Chem. 279*, 11546−11552.
9. Poelarends, G. J., Serrano, H., Person, M. D., Johnson, W. H., Jr., Murzin, A. G., and Whitman, C. P. (2004) Cloning, expression, and characterization of a *cis*-3-chloroacrylic acid dehalogenase: Insights into the mechanistic, structural, and evolutionary relationship between isomer-specific 3-chloroacrylic acid dehalogenases, *Biochemistry 43*, 759−772.
10. Poelarends, G. J., Serrano, H., Johnson, W. H., Jr., and Whitman, C. P. (2004) Stereospecific alkylation of *cis*-chloroacrylic acid dehalogenase by (*R*)-oxirane-2-carboxylate: Analysis and mechanistic implications, *Biochemistry 43*, 7187−7196.
11. de Jong, R. M., Bazzacco, P., Poelarends, G. J., Johnson, W. H., Jr., Kim, Y.-J., Burks, E. A., Serrano, H., Thunnissen, A.-M. W. H., Whitman, C. P., and Dijkstra, B. W. (2007) Crystal structures of native and inactivated *cis*-3-chloroacrylic acid dehalogenase: Structural basis for substrate specificity and inactivation by (*R*)-oxirane-2-carboxylate, *J. Biol. Chem. 282*, 2440−2449.
12. Murzin, A. G. (1996) Structural classification of proteins: New superfamilies, *Curr. Opin. Struct. Biol. 6*, 386−394.
13. Whitman, C. P. (2002) The 4-oxalocrotonate tautomerase family of enzymes: How nature makes new enzymes using a β-α-β structural motif, *Arch. Biochem. Biophys. 402*, 1−13.
14. Poelarends, G. J., and Whitman, C. P. (2004) Evolution of enzymatic activity in the tautomerase superfamily: Mechanistic and structural studies of the 1,3-dichloropropene catabolic enzymes, *Bioorg. Chem. 32*, 376−392.
15. Laemmli, U. K. (1970) Cleavage of structural proteins during the assembly of the head of bacteriophage T4, *Nature 227*, 680−685.
16. Waddell, W. J. (1956) A simple ultraviolet spectrophotometric method for the determination of protein, *J. Lab. Clin. Med. 48*, 311−314.
17. Stamps, S. L., Fitzgerald, M. C., and Whitman, C. P. (1998) Characterization of the role of the amino-terminal proline in the enzymatic activity catalyzed by macrophage migration inhibitory factor, *Biochemistry 37*, 10195−10202.
18. Taylor, A. B., Johnson, W. H., Jr., Czerwinski, R. M., Li, H.-S., Hackert, M. L., and Whitman, C. P. (1999) Crystal structure of macrophage migration inhibitory factor complexed with (*E*)-2-fluoro-*p*-hydroxycinnamate at 1.8 Å resolution: Implications for enzymatic catalysis and inhibition, *Biochemistry 38*, 7444−7452.
19. Johnson, W. H., Jr., Czerwinski, R. M., Stamps, S. L., and Whitman, C. P. (1999) A kinetic and stereochemical investigation of the role of lysine-32 in the phenylpyruvate tautomerase activity catalyzed by macrophage migration inhibitory factor, *Biochemistry 38*, 16024−16033.
20. Gawron, O., Glaid, A. J., and Fondy, T. P. (1961) Stereochemistry of Krebs' cycle hydrations and related reactions, *J. Am. Chem. Soc. 83*, 3634−3640.
21. Englard, S., Britten, J. S., and Listowsky, I. (1967) Stereochemical course of the maleate hydratase reaction, *J. Biol. Chem. 242*, 2255−2259.
22. Knox, W. E., and Pitt, B. M. (1957) Enzymic catalysis of the keto-enol tautomerization of phenylpyruvic acids, *J. Biol. Chem. 225*, 675−688.
23. Blasi, F., Fragomele, F., and Covelli, I. (1969) Thyroidal phenylpyruvate tautomerase. Isolation and characterization, *J. Biol. Chem. 244*, 4864−4870.
24. Ma, Y.-A., Sih, C. J., and Harms, A. (1999) Enzymatic mechanism of thyroxine biosynthesis: Identification of the "lost three-carbon fragment", *J. Am. Chem. Soc. 121*, 8967−8968.
25. Retey, J., Bartl, K., Ripp, E., and Hull, W. E. (1977) Stereospecificity of phenylpyruvate tautomerase. A convenient method for the preparation of chirally labeled phenylpyruvates, *Eur. J. Biochem. 72*, 251−257.
26. Pirrung, M. C., Chen, J., Rowley, E. G., and McPhail, A. T. (1993) Mechanistic and stereochemical study of phenylpyruvate tautomerase, *J. Am. Chem. Soc. 115*, 7103−7110.
27. Rosengren, E., Aman, P., Thelin, S., Hansson, C., Ahlfors, S., Bjork, P., Jacobsson, L., and Rorsman, H. (1997) The macrophage migration inhibitory factor MIF is a phenylpyruvate tautomerase, *FEBS Lett. 417*, 85−88.
28. George, M., and Vaughan, J. H. (1962) In vitro cell migration as a model for delayed hypersensitivity, *Proc. Soc. Exp. Biol. Med. 111*, 514−521.
29. Bloom, B. R., and Bennett, B. (1966) Mechanism of a reaction in vitro associated with delayed-type hypersensitivity, *Science 153*, 80−82.
30. David, J. R. (1966) Delayed hypersensitivity in vitro: Its mediation by cell-free substances formed by lymphoid cell-antigen interaction, *Proc. Natl. Acad. Sci. U.S.A. 56*, 72−77.
31. Leng, L., Metz, C. N., Fang, Y., Xu, J., Donnelly, S., Baugh, J., Delohery, T., Chen, Y., Mitchell, R. A., and Bucala, R. (2003) MIF signal transduction initiated by binding to CD74, *J. Exp. Med. 197*, 1467−1476.
32. Dios, A., Mitchell, R. A., Aljabari, B., Lubetsky, J., O'Conner, K., Liao, H., Senter, P. D., Manoque, K. R., Lolis, E., Metz, C., Bucala, R., Callaway, D. J. E., and Al-Abed, Y. (2002) Inhibition of MIF bioactivity by rational design of pharmacological inhibitors of MIF tautomerase activity, *J. Med. Chem. 45*, 2410−2416.
33. Lubetsky, J., Dios, A., Han, J., Aljabari, B., Ruzsicska, B., Mitchell, R., Lolis, E., and Al-Abed, Y. (2002) The tautomerase active site of macrophage migration inhibitory factor is a potential target for discovery of novel anti-inflammatory agents, *J. Biol. Chem. 277*, 24976−24982.
34. Stamps, S. L., Taylor, A. B., Wang, S. C., Hackert, M. L., and Whitman, C. P. (2000) Mechanism of the phenylpyruvate tautomerase activity of macrophage migration inhibitory factor: Properties of the P1G, P1A, Y95F, and N97A mutants, *Biochemistry 39*, 9671−9678.
35. Suzuki, M., Sugimoto, H., Nakagawa, A., Tanaka, I., Nishihira, J., and Sakai, M. (1996) Crystal structure of the macrophage migration inhibitory factor from rat liver, *Nat. Struct. Biol. 3*, 259−266.
36. Sun, H.-W., Bernhagen, J., Bucala, R., and Lolis, E. (1996) Crystal structure at 2.6 Å resolution of human macrophage migration inhibitory factor, *Proc. Natl. Acad. Sci. U.S.A. 93*, 5191−5196.
37. Lubetsky, J., Swope, M., Dealwis, C., Blake, P., and Lolis, E. (1999) Pro-1 of macrophage migration inhibitory factor functions as a catalytic base in the phenylpyruvate tautomerase activity, *Biochemistry 38*, 7346−7354.
38. Horvat, C. M., and Wolfenden, R. V. (2005) A persistent pesticide residue and the unusual catalytic proficiency of a dehalogenating enzyme, *Proc. Natl. Acad. Sci. U.S.A. 102*, 16199−16202.
39. Poelarends, G. J., Almrud, J. J., Serrano, H., Darty, J. E., Johnson, W. H., Jr., Hackert, M. L., and Whitman, C. P. (2006) Evolution of enzymatic activity in the tautomerase superfamily: Mechanistic and structural consequences of the L8R mutation in 4-oxalocrotonate tautomerase, *Biochemistry 45*, 7700−7708.

40. Peliska, J. A., and O'Leary, M. H. (1991) Preparation and properties of enolpyruvate, *J. Am. Chem. Soc. 113*, 1841−1842.
41. Czerwinski, R. M., Johnson, W. H., Jr., Whitman, C. P., Harris, T. K., Abeygunawardana, C., and Mildvan, A. S. (1997) Kinetic and structural effects of mutations of the catalytic amino-terminal proline in 4-oxalocrotonate tautomerase, *Biochemistry 36*, 14551−14560.
42. O'Brien, P. J., and Herschlag, D. (1999) Catalytic promiscuity and the evolution of new enzymatic activities, *Chem. Biol. 6*, R91−R105.
43. O'Brien, P. J., and Herschlag, D. (2001) Functional interrelationships in the alkaline phosphatase superfamily: Phosphodiesterase activity of *Escherichia coli* alkaline phosphatase, *Biochemistry 40*, 5691−5699.
44. Copley, S. D. (2003) Enzymes with extra talents: Moonlighting functions and catalytic promiscuity, *Curr. Opin. Chem. Biol. 7*, 265−272.
45. Roodveldt, C., and Tawfik, D. S. (2005) Shared promiscuous activities and evolutionary features in various members of the amidohydrolase superfamily, *Biochemistry 44*, 12728−12736.
46. Yew, W. S., Akana, J., Wise, E. L., Rayment, I., and Gerlt, J. A. (2005) Evolution of enzymatic activities in the orotidine 5′-monophosphate decarboxylase suprafamily: Enhancing the promiscuous D-arabino-hex-3-ulose 6-phosphate synthase reaction catalyzed by 3-keto-L-gulonate 6-phosphate decarboxylase, *Biochemistry 44*, 1807−1815.
47. Wang, S. C., Johnson, W. H., Jr., and Whitman, C. P. (2003) The 4-oxalocrotonate tautomerase- and YwhB-catalyzed hydration of 3*E*-haloacrylates: Implications for evolution of new enzymatic activities, *J. Am. Chem. Soc. 125*, 14282−14283.
48. Poelarends, G. J., Serrano, H., Johnson, W. H., Jr., Hoffman, D. W., and Whitman, C. P. (2004) The hydratase activity of malonate semialdehyde decarboxylase: Mechanistic and evolutionary implications, *J. Am. Chem. Soc. 126*, 15658−15659.
49. Wang, S. C., Johnson, W. H., Jr., Czerwinski, R. M., and Whitman, C. P. (2004) Reactions of 4-oxalocrotonate tautomerase and YwhB with 3-halopropiolates: Analysis and implications, *Biochemistry 43*, 748−758.

BI7007189